Physics in Medicine & Biology

IPEM
Institute of Physics and Engineering in Medicine

PAPER • OPEN ACCESS

Experimental validation of daily adaptive proton therapy

To cite this article: Lena Nenoff *et al* 2021 *Phys. Med. Biol.* **66** 205010

View the article online for updates and enhancements.

You may also like

- Three-dimensional tissues using human pluripotent stem cell spheroids as biofabrication building blocks
Haishuang Lin, Qiang Li and Yuguo Lei
- Changes in CYP2C19 enzyme activity evaluated by the [^{13}C]-pantoprazole breath test after co-administration of clopidogrel and proton pump inhibitors following percutaneous coronary intervention and correlation to platelet reactivity
Adrien Harvey, Anil Modak, Ugo Déry et al.
- Acellular implantable and injectable hydrogels for vascular regeneration
Michael R Blatchley and Sharon Gerecht

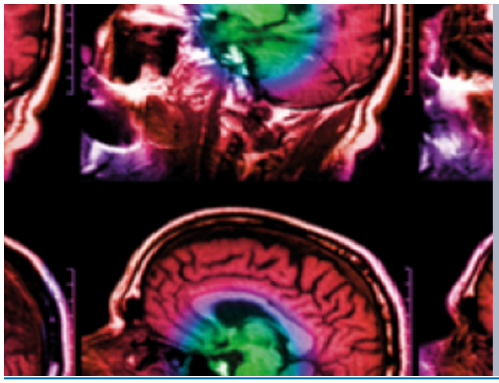

IPEM | IOP
Series in Physics and Engineering in Medicine and Biology

Your publishing choice in medical physics, biomedical engineering and related subjects.

Start exploring the collection–download the first chapter of every title for free.

This content was downloaded from IP address 130.92.245.40 on 03/12/2021 at 16:43

IOP Publishing Phys. Med. Biol. 66 (2021) 205010 https://doi.org/10.1088/1361-6560/ac2b84

Physics in Medicine & Biology

IPEM Institute of Physics and Engineering in Medicine

CrossMark

OPEN ACCESS

RECEIVED
8 May 2021

REVISED
20 September 2021

ACCEPTED FOR PUBLICATION
29 September 2021

PUBLISHED
12 October 2021

Original content from this work may be used under the terms of the Creative Commons Attribution 4.0 licence.

Any further distribution of this work must maintain attribution to the author(s) and the title of the work, journal citation and DOI.

PAPER

Experimental validation of daily adaptive proton therapy

Lena Nenoff[1,2,5,*], **Michael Matter**[1,2,5], **Marjolaine Charmillot**[2], **Serge Krier**[2], **Klara Uher**[2], **Damien Charles Weber**[1,3,4], **Antony John Lomax**[1,2] **and Francesca Albertini**[1,*]

[1] Paul Scherrer Institute, Center for Proton Therapy, Switzerland
[2] Department of Physics, ETH Zurich, Switzerland
[3] Department of Radiation Oncology, University Hospital Zurich, Switzerland
[4] Department of Radiation Oncology, University Hospital Bern, Switzerland
[5] Both authors contributed equally.
[*] Authors to whom any correspondence should be addressed.

E-mail: francesca.albertini@psi.ch **and** lena.nenoff@psi.ch

Keywords: proton therapy, online adaption, end to end test, adaptive therapy, workflow implementation, antropomorphic phantom

Supplementary material for this article is available online

Abstract

Anatomical changes during proton therapy require rapid treatment plan adaption to mitigate the associated dosimetric impact. This in turn requires a highly efficient workflow that minimizes the time between imaging and delivery. At the Paul Scherrer Institute, we have developed an online adaptive workflow, which is specifically designed for treatments in the skull-base/cranium, with the focus set on simplicity and minimizing changes to the conventional workflow. The dosimetric and timing performance of this daily adaptive proton therapy (DAPT) workflow has been experimentally investigated using an in-house developed DAPT software and specifically developed anthropomorphic phantom. After a standard treatment preparation, which includes the generation of a template plan, the treatment can then be adapted each day, based on daily imaging acquired on an in-room CT. The template structures are then rigidly propagated to this CT and the daily plan is fully re-optimized using the same field arrangement, DVH constraints and optimization settings of the template plan. After a dedicated plan QA, the daily plan is delivered. To minimize the time between imaging and delivery, clinically integrated software for efficient execution of all online adaption steps, as well as tools for comprehensive and automated QA checks, have been developed. Film measurements of an end-to-end validation of a multi-fraction DAPT treatment showed high agreement to the calculated doses. Gamma pass rates with a 3%/3 mm criteria were >92% when comparing the measured dose to the template plan. Additionally, a gamma pass rate >99% was found comparing measurements to the Monte Carlo dose of the daily plans reconstructed from the logfile, accumulated over the delivered fractions. With this, we experimentally demonstrate that the described adaptive workflow can be delivered accurately in a timescale similar to a standard delivery.

1. Introduction

Anatomical changes can lead to substantial dose distortions in both conventional and proton radiotherapy treatment (Lomax 2020). This can be best addressed using online adaption, e.g. reoptimizing the therapy based on a 3D image obtained just before the treatment start (see e.g. Raaymakers *et al* 2017, Bernatowicz *et al* 2018, Botas *et al* 2018, Jagt *et al* 2018, Albertini *et al* 2020). In x-ray photon therapy, commercial systems for online adaption have been developed and successfully introduced into the clinics. Online adaption solutions have been realized with MR-Linacs (Raaymakers *et al* 2017) and CT-Linacs (Chamunyonga *et al* 2020) (e.g. Varian's Ethos or RayCare Adaptive Therapy). Given the high sensitivity of proton therapy to such changes, there is currently a large research effort throughout the proton community towards online adaption (e.g. RAPTOR founded by EU Horizon 2020). Simulations of online adaptive proton therapy promise a large benefit for patients (Zhang *et al* 2011, Jagt *et al* 2017,

© 2021 The Author(s). Published on behalf of Institute of Physics and Engineering in Medicine by IOP Publishing Ltd

Wu *et al* 2017, Bernatowicz *et al* 2018, Nenoff *et al* 2019) and many research centers, including ours, are working towards implementing online adaptive proton therapy (e.g Stock *et al* 2017, Albertini *et al* 2020). Nevertheless, to the best knowledge of the authors, online (daily) proton adaption has not yet been deployed clinically.

The benefit of online adaption is threefold. First, the error in the delivered dose due to anatomical changes and positioning uncertainties are reduced. Second, because the errors are reduced, more conformal planning approaches, which would be anatomically un-robust if delivered without adaption, can be chosen (e.g. narrower beam angles and less anatomical-robust planning or smaller CTV-PTV margins). This choice can result in improved organ at risk (OAR) sparing and reduced integral dose (Nenoff *et al* 2019). Third, the image taken just before treatment allows for a dose calculation in the actual patient geometry, which results in a more accurate estimate of the actual dose delivered to the patient. This third point is relevant for both reporting and monitoring the treatment.

In this work, we have developed a comprehensive and clinically applicable workflow for daily adaptive proton therapy (DAPT). The development has focused on simplicity and aims to minimize changes to our conventional patient treatment workflow, with the goal to ease its introduction into the clinic. As such, for this first implementation, we decided to focus on treatments in the nasopharynx, skull base and brain where little or no target or OAR deformations are expected. This allows for rigid structure propagation from the reference image to the daily image, eases quality assurance and speeds up the whole process. Further, we use a dedicated, in-room CT for the daily image acquisition, also greatly simplifying the workflow, as this provides calibrated imaging of proton stopping power of equal quality and geometric fidelity as the original planning CT. Lastly, we use the same clinically validated algorithms for the online plan generation as for a standard treatment plan.

To be able to execute the whole adaption workflow in a safe and fast way, we have developed an integrated software tool called 'ADAPT', which guides the user step-by-step through the workflow of the DAPT treatment. In addition, we have developed a set of QA checks, which we believe allow for a safe execution of this workflow. These QA checks are all fully integrated into ADAPT.

The clinical implementation of any new complex workflow such as DAPT should be tested as close as possible to the clinical scenario, including the delivery and the measurement of the planned dose distribution, in an end-to-end test. To support such clinical tests, sophisticated anthropomorphic phantoms, enabling realistic anatomical changes in a reproducible way, are required. Even though highly desired, such phantoms are rare on the market. Several research centers have therefore worked on in-house solutions. Recently, anthropomorphic phantoms with realistic anatomical changes were built for the pelvis region (Cunningham *et al* 2019, Niebuhr *et al* 2019) and used for an end-to-end test of online adapted treatments in an MRI linac (Bohoudi *et al* 2019, Elter *et al* 2019, Hoffmans *et al* 2020). An anthropomorphic phantom allowing for intrafractional anatomical changes (breathing motion) of the lung and liver has been developed at the Paul Scherrer Institute (PSI) (Perrin *et al* 2017, Colvill *et al* 2020). In addition, a commercial phantom modeling changing brain tumors (Dimitriadis *et al* 2017) is available from CIRS (Computerized Imaging Reference Systems, Inc., Norfolk, USA). Finally, it has been also suggested to 3D-print different anatomical scenarios of the same patient (Ehler *et al* 2014, Kamomae *et al* 2017, Hernandez-Giron *et al* 2019).

In this study, the 'ADAPT' implementation of a DAPT workflow for indications in the head was tested for a three-fraction delivery to a newly developed anthropomorphic phantom designed specifically for experimentally validating adaptive workflows in radiotherapy. The execution time of each workflow step was recorded and the delivered doses of single fraction and 3-fraction DAPT treatments were measured.

The aims of this paper are thus threefold:

1. To perform a comprehensive, end-to-end testing of the whole ADAPT workflow.
2. To give a detailed description of the full ADAPT workflow, its implementation and all aspects of the fully automated, online QA that is integrated into the workflow.
3. To experimentally demonstrate this workflow can be delivered within comparable times to a standard workflow and show that conformal and homogenous doses, even under conditions of varying internal anatomy, can be delivered.

2. Methods

2.1. The DAPT workflow

The complete workflow for our DAPT implementation is shown in figure 1, with the processes in the highlighted boxes being implemented in our in-house developed ADAPT tool. An important part of this is the Plan and Physical QA, a detailed description of which can be found in the supplementary material (available online at stacks.iop.org/PMB/66/205010/mmedia). This full process has been tested in a comprehensive end-to-end test

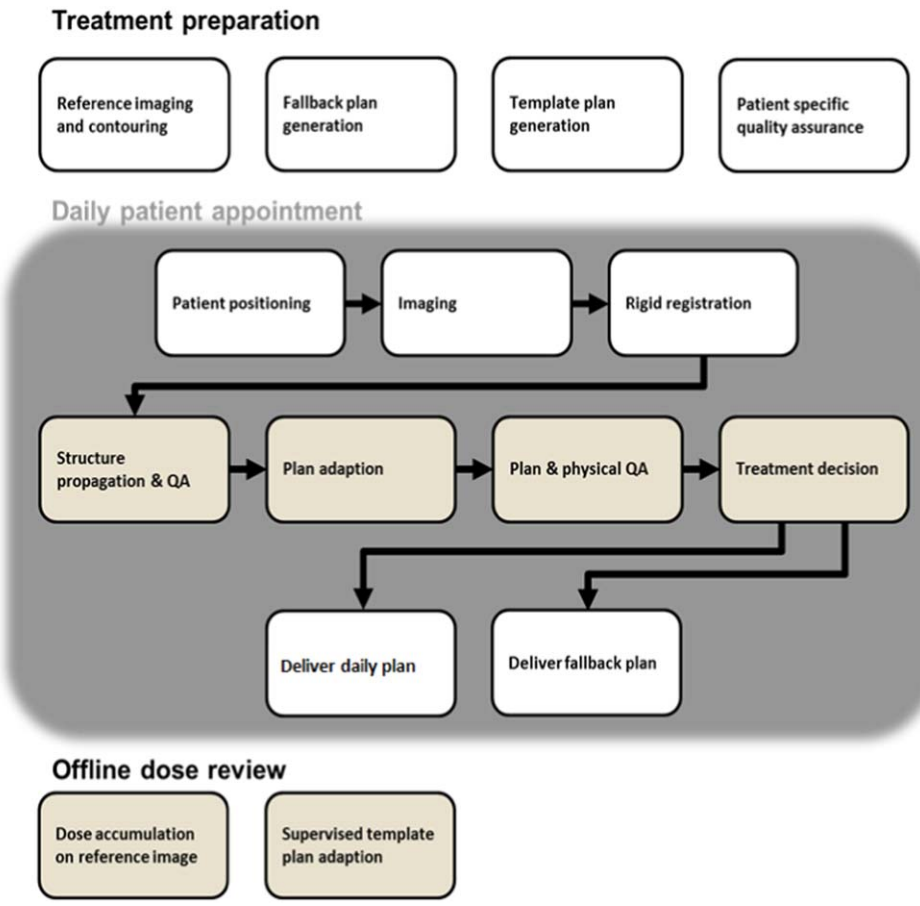

Figure 1. The workflow scheme of the DAPT implementation at PSI. The highlighted boxes represent work steps executed in the newly developed daily adaption tool, ADAPT.

setting using a specifically developed anthropomorphic head phantom, with both dosimetric and timing of the full process being evaluated.

After the reference imaging (planning CT) and contouring, two plans are created, a *template plan* and a *fallback plan*, which both undergo the full clinical and physical QA processes. We define the *template plan* as the target, beam geometry and set of dose constraints that will then be used on a daily basis to re-optimize the dose distribution based on the anatomy of the day (*daily plan*). As the *daily plan* will be adapted to changes in patient anatomy on a daily basis, smaller margins and anatomically unrobust, but conformal beam angles can be used for these (see e.g. Nenoff *et al* 2019). If the *daily plan* passes the clinical and physical QA, it is delivered and reviewed offline after treatment. If necessary, the *template plan* can also be adjusted offline. In contrast, the *fallback plan* is defined to be used if anything goes wrong with the daily adaptive workflow (i.e. on-board imaging is not possible or a QA test of the DAPT workflow fails). As such, the *fallback plan* will typically be different to the *template plan,* being designed using beam angles that are more robust to anatomical changes and using larger PTV margins.

2.2. Anthropomorphic head and neck phantom for DAPT validation

For the end-to-end test of the full DAPT workflow, an anthropomorphic head and neck phantom, which allows for many different internal anatomical configurations, has been developed together with CIRS (figure 2(a)). The phantom is sliced into 5 pieces along the coronal axes. Three of the five coronal slices cross the nasal cavities, which allows the positioning of films or thermoluminescent detectors in close proximity of areas where the anatomy changes. The nasal cavities are accessible and can be filled independently with a mucus-equivalent material. The seven parts of the nasal cavities can be either empty, half filled (cranial or caudal) or completely filled. This results in $4^7 = 16\,384$ different filling possibilities (figure 2(b)). Additionally, the phantom has two fat layers (of 1 and 2 cm thickness) which can be positioned around the neck, to simulate weight changes (figure 2(c)). Moreover, the brain can be filled with different cubes, as for example with different 3D printed tumor inserts (to simulate variations in the tumor size/shape), or with a neutral brain equivalent material (Dimitriadis *et al* 2017) (figure 2(d)). Finally, a cylindrical channel has been drilled through the larynx to the

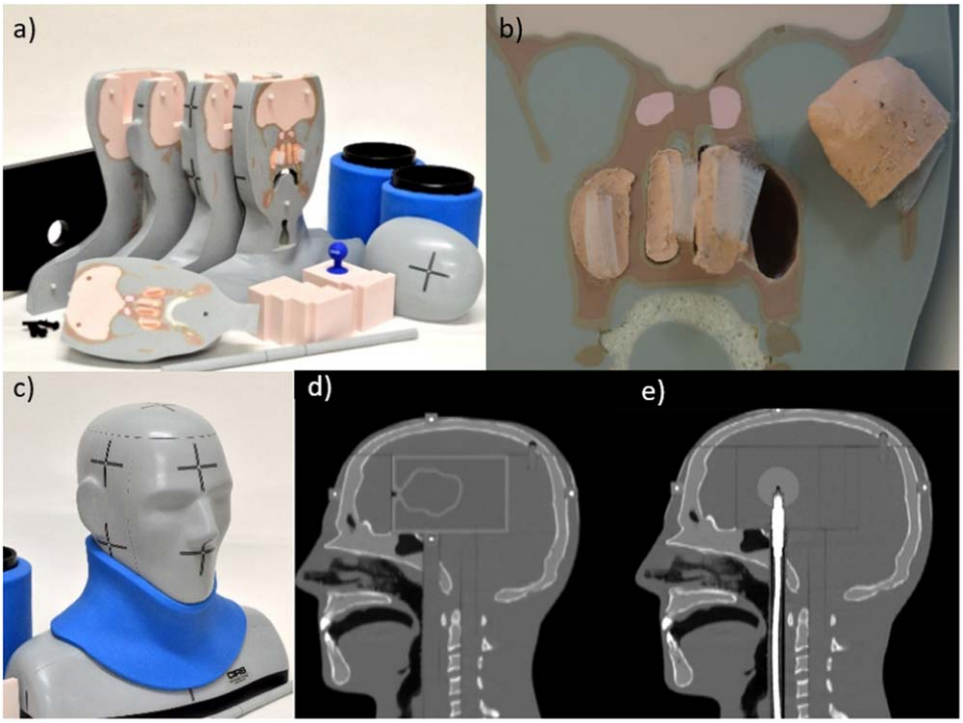

Figure 2. (a) The anthropomorphic head and neck phantom allows for flexible and reproducible anatomical changes. Reproduced with permission from CIRS- Computerized Imaging Reference Systems, Inc. (b) The filling of the nasal cavities can be changed independently with a tissue equivalent mucus material. (c) Fat layers of one and two cm thickness can be placed around the phantom to simulate patient weight changes. Reproduced with permission from CIRS- Computerized Imaging Reference Systems, Inc. (d) Example of an exchange brain tumor insert. Reproduced with permission from CIRS- Computerized Imaging Reference Systems, Inc. (e) A removable rod allows for measurements with an ionization chamber. Reproduced with permission from CIRS- Computerized Imaging Reference Systems, Inc.

brain. This channel allows to measure the dose with an ionization chamber. If this is not needed, it can be filled with a soft-tissue equivalent material (figure 2(e)).

The phantom is constructed from tissue equivalent materials, for which the stopping power has been previously measured (Albertini *et al* 2011). The stopping power of the new mucus material was measured following the same procedure and has been confirmed to match our clinical calibration curve. For the end-to-end test measurements reported here, the phantom has been used with different fillings of the nasal cavities, homogeneous tissue-equivalent brain, a soft-tissue equivalent rod channel filling and no fat layers.

2.3. Treatment preparation

For the treatment preparation, a planning CT of the anthropomorphic phantom with asymmetric, partially filled nasal cavities was acquired, using the standard CT protocol. A realistic tumor volume and OARs (e.g. brainstem, optical structures) were defined in the phantom and checked by an experienced radiation oncologist. As positioning uncertainties are expected to be close to zero for daily adapted treatments (the daily plan is optimized directly on the CT-of-the-day for the patient), a margin of 1 mm around the CTV was added to account for couch motion uncertainty when moving from the in-room CT on rails to the proton Gantry (Nenoff *et al* 2019). As for tumors in the skull base/cranium no intra-fractional motion are expected, the used margin is only dealing with the mechanical uncertainties in the positioning. For other anatomical sites a different margin might be necessary. In addition, to cover range uncertainty scenarios, $\pm 3\%$ scaled HU values are included in the optimization. For the end-to-end tests, a template plan consisting of 3 narrow, conformal beams (field 1: gantry: 30°, couch 0°, field 2: gantry −30°, couch 0°, field 3: gantry 15°, couch 90°) was optimized using dose constraints on critical structures compatible with prescription dose of 66 Gy-RBE delivered in 33 fractions (RBE $= 1.1$). This template plan was then subjected to our standard, clinical patient specific QA procedures (Lomax *et al* 2004).

The template plan is so-called because it is the reference plan used to guide the calculation of the daily (adapted) plan. Subsequently, the daily plan uses the same target (CTV $+$ 1 mm), optimizer, field directions, OAR-DVH constraints and delivery settings as the template plan.

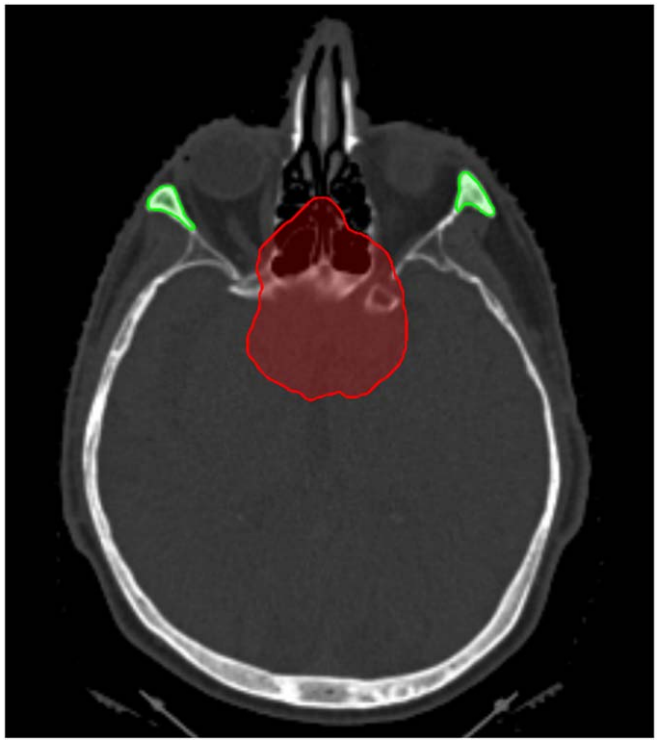

Figure 3. Example of positioning structures (green), small contoured bone parts in close proximity to the target (red), which are used for the structure propagation quality assurance.

In addition, ADAPT requires the following additional steps to be performed during the treatment preparation, described in more detail in the following sections:

- The definition of '*positioning QA structures*' which are used to QA structure propagation from the reference to daily CT.
- The definition of a so-called '*DAPT prescription*' which defines acceptable deviations of dosimetric parameters of the daily plan from the template plan.

2.3.1. Positioning QA structures

These are bony structures in close proximity to the target or in the beam entrance area which are not expected to deform or move relative to the target. A set of these small bony structures are contoured on the reference CT (see example in figure 3). They are used during the structure propagation for a fast automated online QA, where the average HU of these structures is compared between the pair of images, to check the precision of the rigid registration. Already small position deviations would lead to a decrease of the average HU of these structures, which will be detected in automatic checks. These structures also ease a fast visual check of the structure propagation, as small deviations can be more easily identified than using clinical contours that may be in low-contrast areas of the CT.

2.3.2. DAPT prescription

This is defined by the radiation oncologist after the generation of the template plan. For every relevant OAR and target DVH parameter defined and accepted for the *template plan*, acceptable variations of these parameters in the daily plan are defined. In addition, this DAPT prescription also includes maximum tolerable values for global plan parameters such as integral dose and maximum doses inside and outside the target. These tolerances are used for the online plan acceptance of the automatically generated daily plan.

2.4. Daily plan adaption and treatment decision

The DAPT workflow starts with the positioning of the patient on the treatment couch. After positioning, a daily CT image is obtained with our in-room CT on rails (Siemens Healthcare GmbH, Erlangen, Germany) using a specifically developed low-dose CT protocol (supplement 1). The in-room CT is also used for patient positioning in our standard clinical workflow. After imaging, the couch with the patient in treatment position is

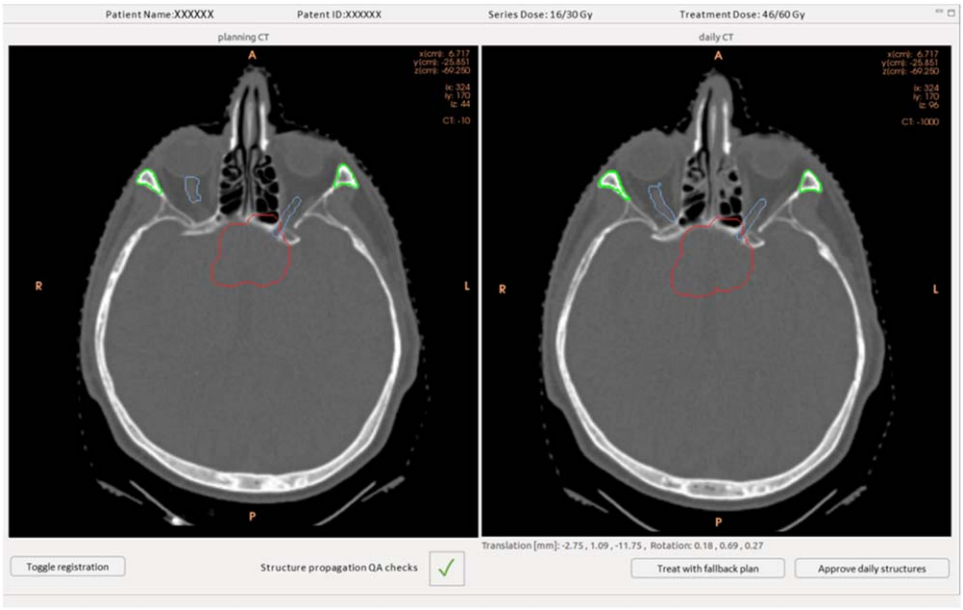

Figure 4. Example of the structure propagation check user interface in ADAPT showing the original structures on the planning CT on the left and the propagated structures on the daily CT on the right. The positioning structures are green, the target red and the OARs blue.

moved to the gantry. After the daily CT acquisition, a 6 degree of freedom 3D–3D rigid registration in a manually chosen region of interest to the reference CT is conducted in VeriSuite (MedCom, Darmstadt, Germany). This registration is visually checked in VeriSuite and the DICOM registration file is sent to ADAPT.

After the daily CT and the corresponding registration file are imported to ADAPT, the reference structures are propagated to the daily CT using the inverse registration vector from VeriSuite. As a QA of the propagated structures, automatic software checks are combined with a brief visual inspection. For the latter, in the user interface (UI) of ADAPT, the reference and daily CTs are displayed side-by-side (figure 4) with all structures relevant for the plan generation and positioning structures displayed. We have found that visual inspection of the positioning structures is useful, even if they are not relevant for the plan optimization, since it is easy to spot if a structure matches or not. In the background, automatic software checks start as soon as the structures are propagated. The results are available and displayed in the UI a couple of seconds after the structure propagation is finished. Details regarding the implemented automated structure and plan QA checks are discussed in more detail in supplement 2. After the visual inspection and the consultation of the automated checks, the daily propagated structures are approved.

Once the propagated structures are available, the fast, GPU supported automatic plan adaption starts in the background (see (Matter *et al* 2019)) which is usually finished once the propagated structures have been approved. The daily plan is newly generated using the template plan as reference for optimization parameters (e.g. field directions, gantry, nozzle and couch position, DVH constraints, optimization and dose calculation algorithm), but with the daily CT and propagated structures as input. A detailed description of the plan generation algorithm for DAPT is given in supplement 3. After the optimization, a machine-readable file for delivering the daily plan is generated.

After the optimization, the daily plan must be clinically accepted. As such, to make this process efficient, tolerances for this decision making are defined *a priori* in the DAPT prescription step (see section 2.3.2). A color-coded table with the DVH parameters with the decision parameters defined in the DAPT prescription is used for this (green for passed, red for failed constraints). A fast decision for a single fraction can usually be made based on this color-coded DAPT prescription table, but nevertheless all DVHs are also available and it is possible to scroll through the dose of the daily plan displayed side-by-side to the template plan (figure 5). In parallel to the clinical plan QA, automatic physical QA checks are conducted in the background as soon as the plan adaption is finished. Details regarding these physical QA checks are described in supplement 2. When the results are available, it is indicated in the UI if all QA has passed, and the plan can then be approved and delivered.

In the proposed online adaptive workflow, it is intended that every day a new daily adapted plan is delivered. This allows the use of smaller margins and fewer fields (Nenoff *et al* 2019), potentially reducing the integral dose to the patient. If the daily plan passes the clinical and physical QA (supplement 2, Matter *et al* 2018), it is delivered to the patient. If not, the fallback plan will be delivered which is calculated following the clinical

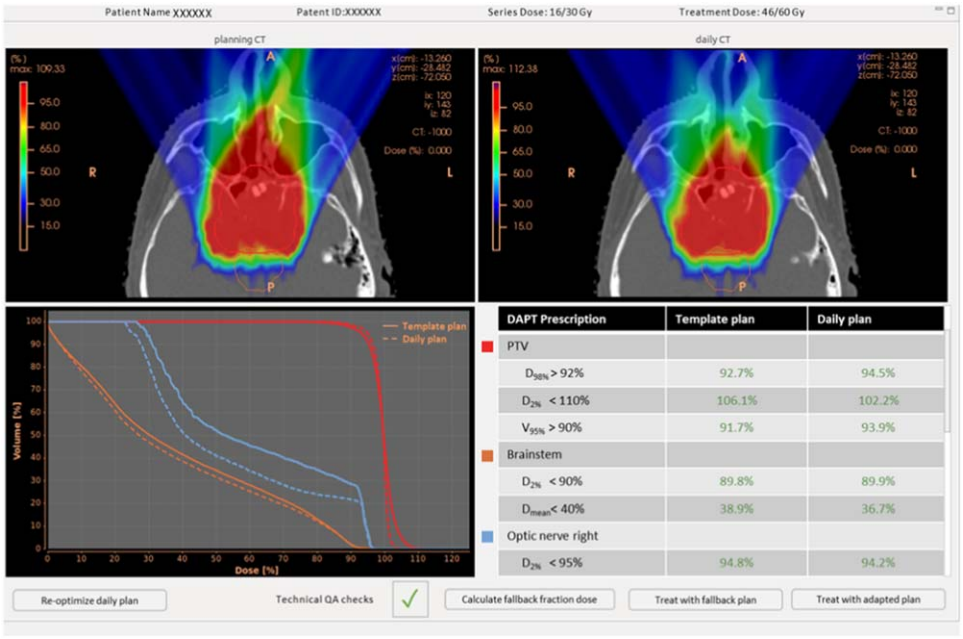

Figure 5. User interface of the Plan QA in ADAPT. More details about the QA results can be displayed when clicking on the Technical QA check.

standards for non-adapted treatments. This ensures that the treatment quality is at least as good as in current clinical practice in the case that the DAPT procedure on a particular day cannot be followed for whatever reason.

2.5. Offline dose review

In addition to the on-line QA described above, an off-line review is also performed. After the delivery of each fraction, the dose is reconstructed based on delivery-log files (Winterhalter *et al* 2019a) and the daily CT using a Monte Carlo (MC) dose calculation (TOPAS version 3.0.p1) providing a highly accurate estimate of the dose delivered to the patient on this fraction. Each such reconstructed dose can then be accumulated on the reference CT over the full course of the treatment, with the reconstructed dose being rigidly shifted to the reference CT using the inverted registration matrix from the structure propagation.

As such, the ADAPT software contains a separate offline dose review environment, where all plan evaluation tools are available. The daily log-file recalculated doses and the accumulated DAPT treatment doses are evaluated and the treatment progress can be monitored. If necessary, changes to the DAPT prescription and the daily optimization constraints can be made, and applied starting with the next fraction. Small changes (OAR-DVH constraint values changes $<5\%$) can be made without a renewed patient specific verification of the template plan, but only if the machine file comparison still passes. This means that no changes in the field angles, or changes which cause differences of more than 10% in total monitor units, are currently allowed. For larger changes, or when re-contouring of the target is necessary, a new template plan needs to be defined.

2.6. Film measurements and analysis

For all experimental validations of the DAPT workflow, Gafchromic EBT3 films (Ashland Advanced Materials, Bridgewter, USA) (LOT 10241701) have been used. The films were calibrated for a dose between 0 and 7 Gy RBE. All films were scanned 24 h after exposure on an EPSON 11000 XL Pro (Epson, Düsseldorf, Germany) following the guidelines defined by GafChromic (Ashland advanced materials). Only the red channel was used. For the experiments, the films were positioned between the coronal slices of the phantom. The white plastic pins for the alignment of the phantom parts (visible in figure 2(a)) were used for placing the films reproducibly inside the phantom. It was previously tested that the acquisition of 10 repeated daily CTs has a negligible impact on the film dose (supplement 1), therefore no correction was applied in the analysis for imaging dose.

As a first test, the DAPT workflow was performed once and applied for a single fraction to the same phantom geometry as the planning CT (only accounting for setup uncertainties). This was followed by a three-fraction treatment to the phantom with different nasal cavity fillings for each fraction. An example slice of the phantom with the different nasal cavity fillings is shown in figure 6. For end-to-end tests, the phantom loaded with films is positioned with the help of positioning lasers and the same positioning devices as for the reference imaging. Apart from the fraction specific CT acquisition, no further image guidance is used.

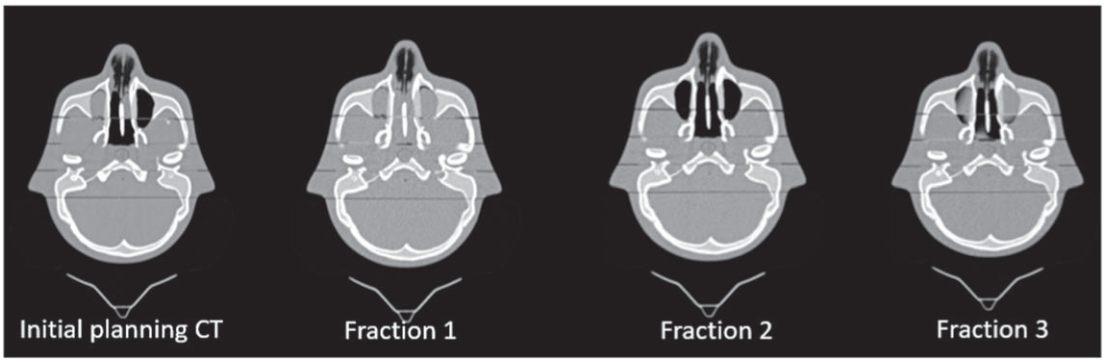

Figure 6. Example CT slices of the 3 different nasal cavity fillings used for the DAPT and standard treatment measurements. The planning CT has an asymmetric nasal cavity filing, the first fraction was completely filed, the second fraction completely empty, the third fraction has asymmetric half-filled nasal cavities (anterior filled, the example CT slice is the border).

Measurements have been compared with the calculated dose distribution in Verisoft (PTW, Freiburg, Germany), which is the software used clinically for patient specific verification measurements at our institute. Dose distributions are normalized individually. A gamma analysis was performed using a threshold of 10% of the prescribed dose and tolerance limits of 3% dose and 3 mm distance to agreement.

Film dosimetry with proton beams is challenging, as the dose response curve of the EBT3 films depends on the linear energy transfer of the protons (Piermattei *et al* 2000, Zhao and Das 2010, Battaglia *et al* 2016, Anderson *et al* 2019). As such, to estimate the quenching effect, we have recalculated the dose of the standard and the template plans with depth-dose curves corrected for quenching and compared it to uncorrected doses. The dose difference in the film slice was homogeneous, so it could be corrected by simply rescaling the film measurements. Indeed, for the multi-field plans applied in this work, the dose at any point is typically applied using a mix of pencil beams and mainly by plateau dose. Consequently, as also the analytical correction method by Zhao and Das (2010) has its own uncertainties, and our measurements are only relative, no additional quenching correction was applied.

2.7. End-to-end tests for single DAPT fraction

For this first experimental validation, the dosimetric accuracy of the DAPT workflow for a single fraction was investigated. A 'daily' CT was acquired, using the same nasal cavity fillings as for the initial planning CT, thus simulating no anatomical changes. Guided by the ADAPT software, the daily CT was registered to the planning CT, structures were propagated, the DAPT plan was generated online, checked automatically (clinical and physical QA) and delivered. The 3%/3 mm gamma pass rate (GPR) between the measured film doses and the calculated dose of (a) the template plan and (b) the daily DAPT plan (optimized on the daily CT) were calculated. The comparison (a) between the measured dose and the template plan shows the difference between the measured and the expected/previously accepted dose, while comparison (b) shows the difference between the measured and the calculated and optimized dose of this day (so validating the dose calculation and DAPT process). The agreement between measured and daily dose (b) is expected to be higher than comparison (a) with the template plan, due to inevitable small differences between the two plans caused by the optimization on the different CTs with slightly changed setup. Additionally, the measured film doses were compared to MC doses reconstructed from the delivery logfile on the daily CT (c). These measurements give information about the dosimetric accuracy of the online DAPT workflow.

2.8. End-to-end tests for a 3-fraction DAPT treatment

As a next step, an end-to-end test of the full ADAPT workflow, simulating the delivery of three separate fractions, each optimized on a different anatomy, was tested. The aim of this test was to measure the accumulated dose for a multi-fractional DAPT treatment. For each fraction, the phantom was positioned after fillings in the nasal cavity were modified (figure 6). The full DAPT workflow has been followed for each of the three fractions. For each workflow step the time was recorded. In this experiment, the dose of all three fractions were delivered to the same film (cumulative dose). The measured cumulative dose distribution is then compared to (a) the reference (template) treatment dose and to (b) the accumulated logfile-reconstructed MC dose on the daily CTs. A 3% dose, 3mm distance to agreement GPR criteria was used. These measurements give information about the dosimetric accuracy of the multi-fraction DAPT treatment.

Table 1. Gamma pass rates (3%/3 mm) of the measurement single DAPT fraction dose compared to the template plan, the daily plan and the logfile MC dose reconstruction on the daily CT.

Measurement position	Template plan	Daily plan	Logfile MC
Distal gradient	94%	98%	100%
Central in tumor	93%	94%	99%
Proximal in tumor	92%	96%	99%

Table 2. Gamma pass rates (3%/3 mm) of the film measurements from the 3-fraction DAPT treatment measurement compared to the template plan and the logfile-MC dose reconstruction accumulated on the planning CT.

Measurement position	Template plan	Logfile MC
Distal gradient	97%	100%
Central in tumor	94%	99%
Proximal in tumor	92%	99%

3. Results

3.1. End-to-end tests for single DAPT fraction

The single DAPT fraction film measurement agreed to the template plan with GPRs between 92% and 94% (table 1). The agreement between the measurement and the daily plan showed an even higher agreement, with GPRs between 94% and 98%. The agreement reduction is due to the intrinsic difference between the template and the daily delivered fraction dose. The agreement between measurement and logfile MC dose reconstruction was excellent, with GPRs being above 99% indicating that logfile-MC dose reconstruction provides the most accurate estimate of the actual daily delivered dose.

3.2. End-to-end tests for a 3-fraction DAPT treatment

Table 2 and figure 7 report the agreement between the measured cumulative dose distribution and the template treatment dose, with 3%/3 mm GPRs between 92% and 97%. In addition, a much improved agreement between measurement and calculation was found for the accumulated logfile MC doses (GPRs >99%). Comparison of the 3-fraction accumulated dose to the template plan and logfile reconstruction is similar to the single fraction measurement, despite the fact that more uncertainties such as film positioning and image registration are involved. As such, a clear experimental benefit has been demonstrated for DAPT treatments, even when delivered in multiple fractions to strongly varying anatomical changes.

3.3. Timing performance

The time measurements for each treatment step started after set-up of the phantom on the treatment table for each fraction. Specific times for each of the three fractions are provided in table 3 and, averaged over all three fractions, in figure 8. On average, a DAPT fraction took 17.9 min, including the plan delivery. This time is similar to a standard treatment delivery, even though many extra steps are needed (rigid registration, structure propagation, optimization and QA) and has been achieved through a fast and efficient software implementation, where all the planning steps are completely integrated and automated. Finally, the patient positioning step is faster for the DAPT plan as no manual repositioning or couch correction are necessary. Additionally, as described by Nenoff *et al* (2019) DAPT plans can potentially consist of fewer beams than standard plans, since they do not have to ensure robustness against anatomical changes, also helping to speed up delivery (figure 8).

4. Discussion

This paper describes a workflow and integrated software solution for online DAPT. The workflow has been tested successfully with a specifically developed phantom in an end-to-end test setting. A DAPT treatment over 3 fractions could be executed efficiently, in a comparable time per fraction as for non-adapted treatments, with the applied doses agreeing well with calculations.

With these tests, we could show that the workflow implemented in the ADAPT software can be safely and efficiently applied, and delivers highly accurate (daily and accumulated) doses, even in the presence of

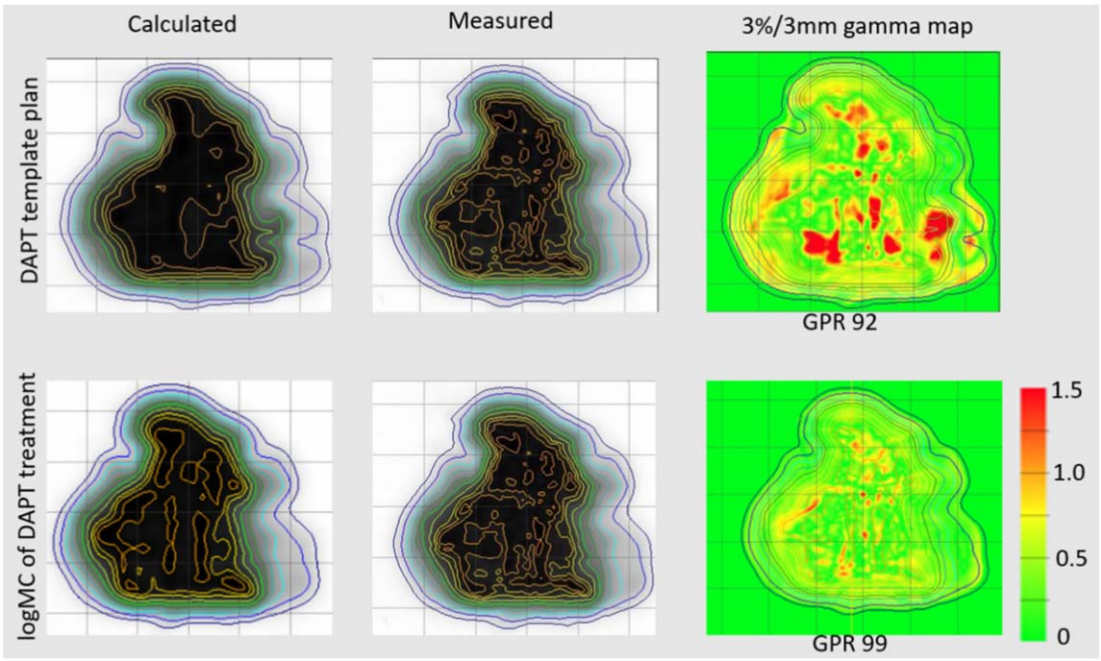

Figure 7. Examples of the calculated (left) and measured (middle) dose distribution and the gamma map (right) in the most proximal phantom slice. Upper row: the measured DAPT treatment dose compared to the DAPT template plan. Lower row: the measured DAPT treatment dose compared to the accumulated logfile Monte Carlo dose.

Table 3. Timing information of the different workflow steps for three DAPT fractions and the average value given in minutes.

Fraction	1	2	3	Average
Imaging	4.0	3.1	3.6	3.6
Rigid registration	2.5	2.4	2.3	2.4
Structure propagation	0.5	0.5	0.5	0.5
Structure QA and plan adaption	1.8	2.0	1.3	1.7
Physical QA and plan QA	0.8	0.6	0.9	0.7
Data transfer and treatment start	0.8	0.9	0.8	0.8
Delivery	7.9	9.4	7.2	8.2
Total	18.4	18.9	16.4	17.9

anatomical changes (figure 7, tables 1 and 2). Nevertheless, differences to the template plan remain, which can be partially accounted for as our DAPT workflow involves a full plan re-optimization of the plan on the daily anatomy. In case of major anatomical differences therefore, dose differences in the DAPT plans of each fraction to that of the template plan are to be expected. Indeed, in the case of a more favorable anatomical situation on a particular fraction (i.e. reduced density heterogeneities along the beam paths) plan quality can even be improved (Nenoff *et al* 2019). This will also manifest itself as a difference in measured dose between the daily delivered and template plans.

Between the measured film dose and the MC dose reconstructed from the delivery logfile we found an excellent agreement (tables 1 and 2, figure 7). This is crucial, as in clinical practice the DAPT fraction dose cannot be verified with measurements before the delivery. Our results show that the logfile MC dose reconstruction gives a very good representation of the actual delivered dose to the patient and can be calculated as an offline, and independent QA directly after the delivery of each fraction (see offline dose review, section 2.5). With this, the delivered dose to the patient is known with a much higher precision than in current clinical practice. Of course, the logfile MC dose can also be recalculated for standard treatments (Winterhalter *et al* 2019b). However, if no daily 3D image is available, the dose can only be reconstructed on the original planning CT, which necessarily ignores any fraction specific anatomical changes. As has been previously demonstrated (Nenoff *et al* 2020), the effect of anatomical changes can be much higher than differences between an analytical or MC dose calculation engine. Therefore, DAPT gives a much better insight into the actual delivered dose than current clinical practice.

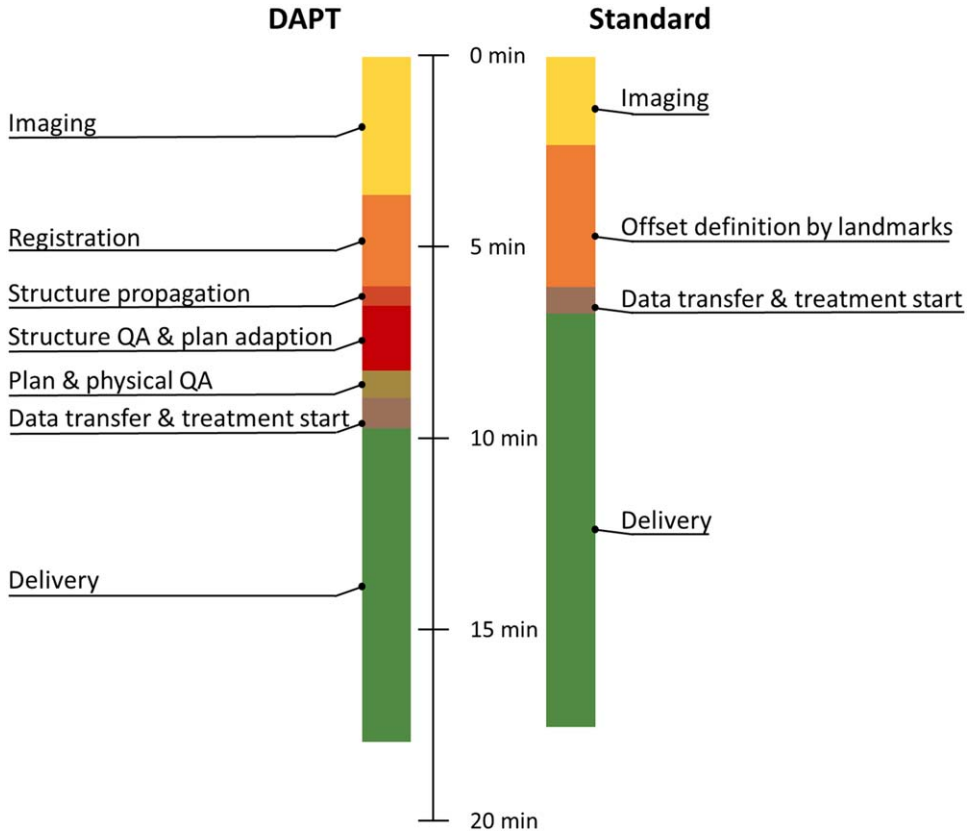

Figure 8. Comparison between the averaged (over three fractions) timing of the workflow steps of the DAPT treatment (left) for a nasal cavity tumor of an anthropomorphic phantom. On the right, the time requirement (average over three fractions) for a non-adapted treatment of the same tumor is shown. The delivery time of the non-adapted treatment is slightly longer since more fields are necessary to create a plan that is robust enough against anatomical changes.

As we have experimentally verified a treatment of only three fractions, large anatomical changes (in the nasal cavities) between each fraction have been considered. The alternative to an online daily adaptive therapy, currently used in the clinic, consist of an off-line plan adaptation triggered by the detection of a dose detriment caused by anatomical changes (Müller *et al* 2015, Hoffmann *et al* 2017, Placidi *et al* 2017, Stützer *et al* 2017). However, such off-line adaptation is time consuming (sometimes taking days depending on the complexity of the plan and associated QA) and the anatomy may have changed again by the next fraction (Bobić *et al* 2021). In our clinic, we have indeed observed such drastic day-to-day changes for some patients treated in the sinus.

The time measurements of our workflow showed that the treatment time for a DAPT fraction could be very similar to that of our conventional clinical workflow. There are however some limitations to these time measurements. For instance, no QA check values were outside tolerance and all DVH parameters of the daily plan were within the DAPT prescription. If something goes wrong however, and any values are outside the tolerances defined in the *DAPT prescription*, longer treatment times could of course result. Nevertheless, it is interesting to note that all plan and other QA tests of the ADAPT procedure passed in these tests despite major anatomical changes between fractions.

The DAPT workflow that we have implemented and described here is deliberately simple due to the following choices:

- Base the daily adaption on in-room CT.
- Restrict usage to anatomical regions where rigid registration is sufficient.
- Use the same algorithms for the daily plan generation as for conventional planning.

Much work has been reported on enabling online adaption in proton therapy based on mobile CT (Sun *et al* 2018), CBCT (Kurz *et al* 2016a, 2016b, Botas *et al* 2018, Alcorn *et al* 2020, Lalonde *et al* 2020) or MR images (Koivula *et al* 2016). Extending to CBCT based adaption would greatly widen the applicability of online adaption in proton therapy, even if a number of proton facilities also now have in-room CT capabilities. Using the in-room CT however provides direct access to CT data providing similar HU to stopping power conversion

accuracy as in the normal planning process, without the need for image processing or correction strategies as is necessary for CBCT. Further, there are no problems with a limited field of view as there is for some CBCTs. Indeed, as the daily image is not needed to manually contour OARs, a high soft tissue contrast is not required and consequently the CT current can be reduced. We have found that dose calculation and rigid registration performance did not change for CTs obtained with the low-dose protocol described in supplement 1, whilst this reduced the imaging dose by a factor of three and significantly reduced imaging time. Nevertheless, DAPT will inevitably increase imaging dose, due to the need of acquiring a daily CT. On the other hand, this increase in imaging dose can be the largely compensated by a reduction of the integral dose to healthy tissue, which can be achieved with DAPT by reducing the target margin and potentially through the use of new field arrangements (Nenoff *et al* 2019). MR based adaption would elegantly remove any worries about daily imaging dose through CT/CBCT imaging. However, proton therapy facilities with online MR guidance, although being investigated (Raaymakers *et al* 2008, Oborn *et al* 2017), is far from being clinically available.

Perhaps the clearest limitation of the initial implementation of DAPT described here is its restriction to anatomical sites which we assume only change in a rigid way. Any non-rigid anatomical changes have to be addressed in an offline adaption, based on an off-line MRI or high-quality CT acquisition where new structures can be defined and a new template plan optimized. Obviously, the benefit and applications for adaptive therapy would increase enormously if applied to anatomical regions which deform non-rigidly. However, there are large uncertainties associated with deformable image registration, making an efficient quality assurance of their performance challenging. As such, clinical online adaptive workflows in x-ray therapy rely on manual contouring, or at least manually correcting the automatically propagated structures (Lamb *et al* 2017, Raaymakers *et al* 2017), which is currently the most time consuming step. As such, we have deliberately decided in this first DAPT implementation to restrict our choice of indications to patients with tumors in the skull base, nasal cavities and cranium where no organ and target deformations are expected. Although the applications of DAPT may appear to be restricted in these regions, clinical benefits are still expected (van de Water *et al* 2016, Nenoff *et al* 2019, Lalonde *et al* 2021). In addition, by taking this approach, we have been able to develop a simple and practical DAPT workflow with which we can gain invaluable clinical experience with daily adaptive treatments. Nevertheless, we are also working on expanding this workflow to include deformable registration in the future (Nenoff *et al* 2021).

An important part of our implementation is the use of identical planning, dose calculation and optimization algorithms for the daily adaption as used in our standard planning, of all which have been clinically validated and proven over our many years of clinical operation. Other groups are taking a different approach, e.g. by deliberately limiting the changes between the reference and the daily plan in order to simplify the QA problem. For instance, in the work of Bernatowicz *et al* (2018) and Jagt *et al* (2017) the daily adaptive process aimed at preserving the daily dose as close to that of the reference plan as possible—a process called dose restoration. Alternatively, (Botas *et al* 2018) have investigated an online adaption method, which changes spot energies and weights based on localized anatomical changes, whilst preserving the actual spot list of the verified reference plan. Whilst such approaches have some benefits, on the downside, these restrictions can potentially limit the benefit of the adaption process. As shown previously (Nenoff *et al* 2019), some daily changes in anatomy can provide advantageous geometrical conditions for planning and treatment. For instance, improved dose conformity and somewhat improved critical organ sparing could be achieved in some nasopharynx tumors when the nasal cavities are filled compared to empty, due to the reduced degradation of the Bragg peak. Such effects are expected to be even larger when applying DAPT to deformable anatomies, where the shape and relationship of critical structures to the target volume can change considerably, not to mention potential changes in the tumor volume itself.

Due to time reasons, the DAPT plans are optimized with a simple but fast analytical algorithm. Especially in areas with large density heterogeneities, analytical algorithms have a limited precision (Schuemann *et al* 2014, Maes *et al* 2018). However, previous studies showed that the analytical dose calculation algorithm used here has a high agreement with MC calculations, also in areas with high density heterogeneities such as the nasal cavities or even in lung (Winterhalter *et al* 2019b). Additionally, we have previously shown that anatomical changes have a larger impact on the dose distribution than calculation uncertainties, and a DAPT approach is still beneficial to the patients even if optimized with analytical algorithms (Nenoff *et al* 2020). As time is critical in online adaption and the analytical dose agrees within widely accepted clinical acceptance criteria for Gamma analysis (tables 1 and 2), an online analytical optimization, combined with automated physical QA and off-line logfile-MC calculations, would be beneficial for the patient. The excellent agreement between logfile-MC and measured dose makes it a good representation of the actual delivered dose. If the logfile-MC based dose reconstruction, shows relevant deviations from the daily plan, these dose differences could be quantified and considered as a previously delivered dose in the DAPT plan optimization of the next day. With this, dose deviations from the delivery can be compensated for as part of the DAPT workflow (Matter *et al* 2020).

Important work nevertheless remains to be done to extend the daily online adaption to more patient indications. The most important extension is the integration of deformable image registration into the DAPT workflow and the development of the necessary QA tools for deformable image registration. Also, the extension to other imaging modalities, most importantly cone beam CT, is important to enable a more general application of daily online adaption in proton therapy. Finally, although the described plan adaption algorithm is simple, fast and effective (as long as the volumes do not change) for online adaption with changing target structures and OARs, more sophisticated algorithms may be useful, such as a Pareto optimal plan according to a planning goal 'wishlist' as investigated by Jagt *et al* (2018). Furthermore, if the changes in the daily plan get larger, more comprehensive plan QA strategies need to be developed. Nevertheless, we believe that the described DAPT process is the correct approach to go forward to gain clinical experience with daily treatment adaption, if only on a limited set of indications. This will greatly accelerate development and ease the way for the clinical introduction of the necessary extensions.

5. Conclusion

An online adaptive workflow was designed and a software solution including comprehensive QA checks was developed to treat patients with cranial indications. For experimental validation, a comprehensive end-to-end test of a highly efficient workflow was performed and showed that such a workflow is practical, fast, safe and accurate. The workflow is currently being prepared for clinical commissioning.

Acknowledgments

We acknowledge Swiss National Science Foundation for founding this work in within the project 'Towards daily adaption at PSI', grant number: 320030_165961. We thank Michele Togno for SPR measurements.

ORCID iDs

Lena Nenoff https://orcid.org/0000-0002-7468-835X
Michael Matter https://orcid.org/0000-0002-2612-3207

References

Albertini F, Casiraghi M, Lorentini S, Rombi B and Lomax A J 2011 Experimental verification of IMPT treatment plans in an anthropomorphic phantom in the presence of delivery uncertainties *Phys. Med. Biol.* **56** 4415–31

Albertini F, Matter M, Nenoff L, Zhang Y and Lomax A 2020 Online daily adaptive proton therapy *Br. J. Radiol.* **92** 20190594

Alcorn S R *et al* 2020 Low-dose image-guided pediatric CNS radiation therapy: final analysis from a prospective low-dose cone-beam CT protocol from a multinational pediatrics consortium *Technol. Cancer Res. Treat.* **19** 1–8

Anderson S E, Grams M P, Wan Chan Tseung H, Furutani K M and Beltran C J 2019 A linear relationship for the LET-dependence of gafchromic EBT3 film in spot-scanning proton therapy *Phys. Med. Biol.* **64** 055015

Ashland advanced materials Efficient protocols for accurate radiochromic film calibration and dosimetry (http://www.gafchromic.com/documents/Efficient%20Protocols%20for%20Calibration%20and%20Dosimetry.pdf)

Battaglia M C, Schardt D, Espino J M, Gallardo M I, Cortés-Giraldo M A, Quesada J M, Lallena A M, Miras H and Guirado D 2016 Dosimetric response of radiochromic films to protons of low energies in the bragg peak region *Phys. Rev. Accel. Beams* **19** 064701

Bernatowicz K, Geets X, Barragan A, Janssens G, Souris K and Sterpin E 2018 Feasibility of online IMPT adaptation using fast, automatic and robust dose restoration *Phys. Med. Biol.* **63** 085018

Bobić M, Lalonde A, Sharp G C, Grassberger C, Verburg J M, Winey B A, Lomax A J and Paganetti H 2021 Comparison of weekly and daily online adaptation for head and neck intensity-modulated proton therapy *Phys. Med. Biol.* **66** 055023

Bohoudi O, Lagerwaard F J, Bruynzeel A M E, Niebuhr N I, Johnen W, Senan S, Slotman B J, Pfaffenberger A and Palacios M A 2019 End-to-end empirical validation of dose accumulation in MRI-guided adaptive radiotherapy for prostate cancer using an anthropomorphic deformable pelvis phantom *Radiother. Oncol.* **141** 200–7

Botas P, Kim J, Winey B and Paganetti H 2018 Online adaption approaches for intensity modulated proton therapy for head and neck patients based on cone beam CTs and Monte Carlo simulations *Phys. Med. Biol.* **64** 015004

Chamunyonga C, Edwards C, Caldwell P, Rutledge P and Burbery J 2020 The impact of artificial intelligence and machine learning in radiation therapy: considerations for future curriculum enhancement *J. Med. Imaging Radiat. Sci.* **51** 214–20

Colvill E *et al* 2020 Anthropomorphic phantom for deformable lung and liver CT and MR imaging for radiotherapy *Phys. Med. Biol.* **65** 07NT02

Cunningham J M, Barberi E A, Miller J, Kim J P and Glide-Hurst C K 2019 Development and evaluation of a novel MR-compatible pelvic end-to-end phantom *J. Appl. Clin. Med. Phys.* **20** 265–75

Dimitriadis A, Palmer A L, Thomas R A S, Nisbet A and Clark C H 2017 Adaptation and validation of a commercial head phantom for cranial radiosurgery dosimetry end-to-end audit *Br. J. Radiol.* **90** 1–9

Ehler E D, Barney B M, Higgins P D and Dusenbery K E 2014 Patient specific 3D printed phantom for IMRT quality assurance *Phys. Med. Biol.* **59** 5763–73

Elter A, Dorsch S, Mann P, Runz A, Johnen W, Spindeldreier C K, Klüter S and Karger C P 2019 End-to-end test of an online adaptive treatment procedure in MR-guided radiotherapy using a phantom with anthropomorphic structures *Phys. Med. Biol.* **64** 225003

Hernandez-Giron I, den Harder J M, Streekstra G J, Geleijns J and Veldkamp W J H 2019 Development of a 3D printed anthropomorphic lung phantom for image quality assessment in CT *Phys. Med.* **57** 47–57
Hoffmann L, Alber M, Jensen M F, Holt M I and Møller D S 2017 Adaptation is mandatory for intensity modulated proton therapy of advanced lung cancer to ensure target coverage *Radiother. Oncol.* **122** 400–5
Hoffmans D, Niebuhr N, Bohoudi O, Pfaffenberger A and Palacios M 2020 An end-to-end test for MR-guided online adaptive radiotherapy *Phys. Med. Biol.* **65** 125012
Jagt T, Breedveld S, van Haveren R, Heijmen B and Hoogeman M 2018 An automated planning strategy for near real-time adaptive proton therapy in prostate cancer *Phys. Med. Biol.* **63** 135017
Jagt T, Breedveld S, van de Water S, Heijmen B and Hoogeman M 2017 Near real-time automated dose restoration in IMPT to compensate for daily tissue density variations in prostate cancer *Phys. Med. Biol.* **62** 4254
Kamomae T *et al* 2017 Three-dimensional printer-generated patient-specific phantom for artificial *in vivo* dosimetry in radiotherapy quality assurance *Phys. Med.* **44** 205–11
Koivula L, Wee L and Korhonen J 2016 Feasibility of MRI-only treatment planning for proton therapy in brain and prostate cancers: dose calculation accuracy in substitute CT images *Med. Phys.* **43** 4634–42
Kurz C *et al* 2016a Investigating deformable image registration and scatter correction for CBCT-based dose calculation in adaptive IMPT *Med. Phys.* **43** 5636–46
Kurz C, Nijhuis R, Reiner M, Ganswindt U, Thieke C, Belka C, Parodi K and Landry G 2016b Feasibility of automated proton therapy plan adaptation for head and neck tumors using cone beam CT images *Radiat. Oncol.* **11** 1–9
Lalonde A, Bobić M, Winey B, Verburg J, Sharp G C and Paganetti H 2021 Anatomic changes in head and neck intensity-modulated proton therapy: comparison between robust optimization and online adaptation *Radiother. Oncol.* **159** 39–47
Lalonde A, Winey B, Verburg J, Paganetti H and Sharp G C 2020 Evaluation of CBCT scatter correction using deep convolutional neural networks for head and neck adaptive proton therapy *Phys. Med. Biol.* **65** 245022
Lamb J *et al* 2017 Online adaptive radiation therapy: implementation of a new process of care *Cureus* **9** e1618
Lomax A J 2020 Proton therapy special feature: review article myths and realities of range uncertainty *Br. J. Radiol.* **93** 1–9
Lomax A J *et al* 2004 Treatment planning and verification of proton therapy using spot scanning: initial experiences *Med. Phys.* **31** 3150–7
Maes D, Saini J, Zeng J, Rengan R, Wong T and Bowen S R 2018 Advanced proton beam dosimetry: II. Monte Carlo versus pencil beam-based planning for lung cancer *Trans. Lung Cancer Res.* **7** 114–21
Matter M, Nenoff L, Marc L, Weber D C, Lomax A J and Albertini F 2020 Update on yesterday's dose-Use of delivery log-files for daily adaptive proton therapy (DAPT) *Phys. Med. Biol.* **65** 195011
Matter M, Nenoff L, Meier G, Weber D C, Lomax A J and Albertini F 2018 Alternatives to patient specific verification measurements in proton therapy: a comparative experimental study with intentional errors *Phys. Med. Biol.* **63** 205014
Matter M, Nenoff L, Meier G, Weber D C, Lomax A J and Albertini F 2019 Intensity modulated proton therapy plan generation in under ten seconds *Acta Oncol.* **58** 1435–9
Meier G, Besson R, Nanz A, Safai S and Lomax A J 2015 Independent dose calculations for commissioning, quality assurance and dose reconstruction of PBS proton therapy *Phys. Med. Biol.* **60** 2819–36
Müller B S, Duma M N, Kampfer S, Nill S, Oelfke U, Geinitz H and Wilkens J J 2015 Impact of interfractional changes in head and neck cancer patients on the delivered dose in intensity modulated radiotherapy with protons and photons *Phys. Med.* **31** 266–72
Nenoff L *et al* 2021 Dosimetric influence of deformable image registration uncertainties on propagated structures for online daily adaptive proton therapy of lung cancer patients *Radiother. Oncol.* **159** 136–43
Nenoff L *et al* 2020 Daily adaptive proton therapy: is it appropriate to use analytical dose calculations for plan adaption? *Int. J. Radiat. Oncol. Biol. Phys.* **107** 747–55
Nenoff L, Matter M, Hedlund Lindmar J, Weber D C, Lomax A J and Albertini F 2019 Daily adaptive proton therapy—the key to innovative planning approaches for paranasal cancer treatments *Acta Oncol.* **58** 1423–8
Niebuhr N I, Johnen W, Echner G, Runz A, Bach M, Stoll M, Giske K, Greilich S and Pfaffenberger A 2019 The ADAM-pelvis phantom—an anthropomorphic, deformable and multimodal phantom for MRgRT *Phys. Med. Biol.* **64** 04NT05
Oborn B M, Dowdell S, Metcalfe P E, Crozier S, Mohan R and Keall P J 2017 Future of medical physics: real-time MRI-guided proton therapy *Med. Phys.* **44** e77–90
Perrin R L *et al* 2017 An anthropomorphic breathing phantom of the thorax for testing new motion mitigation techniques for pencil beam scanning proton therapy *Phys. Med. Biol.* **62** 2486–504
Piermattei A *et al* 2000 Radiochromic film dosimetry of a low energy proton beam *Med. Phys.* **27** 1655–60
Placidi L, Bolsi A, Lomax A J, Schneider R A, Malyapa R, Weber D C and Albertini F 2017 The effect of anatomical changes on pencil beam scanned proton dose distributions for cranial and extra cranial tumors *Int. J. Radiat. Oncol. Biol. Phys.* **97** 616–23
Raaymakers B W *et al* 2017 First patients treated with a 1.5 T MRI-Linac: clinical proof of concept of a high-precision, high-field MRI guided radiotherapy treatment *Phys. Med. Biol.* **62** L41–50
Raaymakers B W, Raaijmakers A J E and Lagendijk J J W 2008 Feasibility of MRI guided proton therapy: magnetic field dose effects related content feasibility of MRI guided proton therapy: magnetic field dose effects *Phys. Med. Biol.* **53** 5615
Schuemann J, Dowdell S, Grassberger C, Min C H and Paganetti H 2014 Site-specific range uncertainties caused by dose calculation algorithms for proton therapy *Phys. Med. Biol.* **59** 4007–31
Stock M *et al* 2017 The technological basis for adaptive ion beam therapy at MedAustron: status and outlook *Z. Med. Phys.* **28** 196–210
Stützer K, Jakobi A, Bandurska-Luque A, Barczyk S, Arnsmeyer C, Löck S and Richter C 2017 Potential proton and photon dose degradation in advanced head and neck cancer patients by intratherapy changes *J. Appl. Clin. Med. Phys.* **18** 104–13
Sun B, Yang D, Lam D, Zhang T, Dvergsten T, Bradley J, Mutic S and Zhao T 2018 Toward adaptive proton therapy guided with a mobile helical CT scanner *Radiother. Oncol.* **129** 479–85
van de Water S, van Dam I, Schaart D R, Al-Mamgani A, Heijmen B J M and Hoogeman M S 2016 The price of robustness; impact of worst-case optimization on organ-at-risk dose and complication probability in intensity-modulated proton therapy for oropharyngeal cancer patients *Radiother. Oncol.* (https://doi.org/10.1016/j.radonc.2016.04.038)
Winterhalter C, Meier G, Oxley D, Weber D C, Lomax A J and Safai S 2019a Log file based Monte Carlo calculations for proton pencil beam scanning therapy *Phys. Med. Biol.* **64** 035014
Winterhalter C *et al* 2019b Evaluation of the ray-casting analytical algorithm for pencil beam scanning proton therapy *Phys. Med. Biol. Biol.* **64** 065021
Wu R Y *et al* 2017 Intensity-modulated proton therapy adaptive planning for patients with oropharyngeal cancer *Int. J. Part. Ther.* **4** 26–34
Zhang M, Westerly D C and Mackie T R 2011 Introducing an on-line adaptive procedure for prostate image guided intensity modulate proton therapy *Phys. Med. Biol.* **56** 4947–65
Zhao L and Das I J 2010 Gafchromic EBT film dosimetry in proton beams *Phys. Med. Biol.* **55** 5617